JOURNAL OF CLINICAL MICROBIOLOGY, Dec. 2001, p. 4413–4419 Vol. 39, No. 12
0095-1137/01/$04.00+0 DOI: 10.1128/JCM.39.12.4413–4419.2001

New LightCycler PCR for Rapid and Sensitive Quantification of Parvovirus B19 DNA Guides Therapeutic Decision-Making in Relapsing Infections

TIMM C. HARDER,[1]* MARKUS HUFNAGEL,[2]† KATRIN ZAHN,[1] KARIN BEUTEL,[2] HEINZ-JOSEF SCHMITT,[2]‡ UWE ULLMANN,[1] AND PETER RAUTENBERG[1]

Department of Medical Microbiology and Virology[1] and University Children's Hospital,[2] Christian-Albrechts University, Kiel, Germany

Received 27 November 2000/Returned for modification 20 March 2001/Accepted 27 September 2001

Detection of parvovirus B19 DNA offers diagnostic advantages over serology, particularly in persistent infections of immunocompromised patients. A rapid, novel method of B19 DNA detection and quantification is introduced. This method, a quantitative PCR assay, is based on real-time glass capillary thermocycling (LightCycler [LC]) and fluorescence resonance energy transfer (FRET). The PCR assay allowed quantification over a dynamic range of over 7 logs and could quantify as little as 250 B19 genome equivalents (geq) per ml as calculated for plasmid DNA (i.e., theoretically ≥5 geq per assay). Interrater agreement analysis demonstrated equivalence of LC-FRET PCR and conventional nested PCR in the diagnosis of an active B19 infection (kappa coefficient = 0.83). The benefit of the new method was demonstrated in an immunocompromised child with a relapsing infection, who required an attenuation of the immunosuppressive therapy in addition to repeated doses of immunoglobulin to eliminate the virus.

The human erythrovirus B19, a member of the family *Parvoviridae*, causes a broad and seemingly expanding spectrum of disorders (7, 12, 23, 44). The clinical picture depends on the immune status and age of the patient (14, 36, 43). Parvovirus B19 shows a remarkable tropism for erythroid progenitor cells in the bone marrow, which is partly based on binding to its receptor, the blood group P antigen (6). Viral replication, and possibly also the induced immune response, interferes with physiological functions and loss of the erythroid progenitor cells, resulting in a usually subclinical reticulocytopenia (8). In patients with an underlying hematologic disorder and high blood cell turnover (e.g., hemolytic anemia), transient aplastic anemia may ensue. Immunocompromised patients, who have an increased risk of developing a persistent B19 infection, are threatened by a chronic reticulocytopenic anemia, also known as pure red cell anemia (2, 8).

Diagnosis of uncomplicated cases of acute B19 infection (fifth disease or arthropathy) is usually clinically based and can be accomplished by detection of specific immunoglobulin M (IgM) antibodies except in immunocompromised patients, who are prone to persistent infection and who may generate IgM-specific B19 antibodies less reliably (7, 19). Likewise, specific IgG is not a reliable marker for discriminating a reconvalescent status from chronic persistent infection (35), although recent data indicate that IgG antibodies specific for nonstructural protein 1 (NS-1) of B19 are more frequently associated with persistent infection (24). Detection of DNA by hybridization or PCR has been reported to be superior in the diagnosis of prenatal B19 infections and in children with oncologic or hematologic disorders (5, 11, 34). Several qualitative and quantitative PCR methods targeting different regions of the parvovirus genome have been published (1, 4, 9, 10, 13, 15, 17, 22, 25, 40). These PCR approaches are based on conventional block thermocycling and combined single-round PCRs with subsequent oligohybridization or use a nested format.

The recently developed LightCycler (LC) DNA amplification technology (Roche Diagnostics, Mannheim, Germany) combines rapid glass capillary thermal cycling with real-time microvolume fluorescence monitoring (47). Detection of amplicons is achieved during the run in real time. Melting point analysis of the amplicons at the end of the run is used as a specificity control when the fluorochrome SYBR green is used for detection of double-stranded DNA. Alternatively, specificity can be tested during the run by using two target-specific hybridization probes which utilize fluorescence resonance energy transfer (FRET) to generate a measurable signal. In the latter case, two oligonucleotide probes (HybProbe) bind to immediately adjacent regions of the respective amplicon. The upstream probe (referred to as the probe) is labeled at its 3′ end with fluorescein, while the 5′ end of the downstream probe (referred to as the anchor) is labeled with either of the fluorochromes LC-Red 640 and LC-Red 705. To avoid elongation by the *Taq* polymerase, the anchor is 3′ phosphorylated. When it is ensured that the probe and anchor are spaced no more than five nucleotides apart, simultaneous binding to the specific target generates an amplified signal which is detected fluorometrically.

In the present study, we introduced a rapid and sensitive PCR assay for the quantification of parvovirus B19 DNA, which is based on LC-FRET technology. Up to 25 samples can be quantitatively analyzed within 45 min. The quantification

* Corresponding author. Present address: Food and Veterinary Diagnostic Laboratory, Max-Eyth Strasse 5, D-24537 Neumuenster, Germany. Phone: 49 4321 904 766. Fax: 49 4321 766 619. E-mail: timm.harder@lvua-sh.de.

† Present address: Channing Laboratory, Brigham and Women's Hospital, Department of Medicine, Boston, MA 02115.

‡ Present address: Center for Preventive Pediatrics, Department of Pediatric Infectious Diseases, University Children's Hospital, Johannes-Gutenberg University, D-55101 Mainz, Germany.

TABLE 1. Primer pairs and block cycler programs for PCR amplification of B19 DNA

Primer	Sequence[a]	Position[b]	Product length (bp)	Cycling	No. of cycles
NS-1a	CCG CCA AGT ACA GGA AAA AC	1420–1439	229	95°C, 20 s 58°C, 20 s 72°C, 30 s	35
NS-1a′	CAG CTA CAC TTC CAC GCA	1648–1631			
NS-1b	AAT GAA AAC TTT CCA TTT AAT GAT GTA G	1498–1525	99 (nested)	95°C, 20 s 56°C, 20 s 72°C, 20 s	35
NS-1b′	**G**AT GGC TTT TGC AGC TTC TAC	1595–1576			
VP-a	**CA**G ATG GGG TTT GCA TCA G	4459–4477	319	95°C, 20 s 57°C, 20 s 72°C, 20 s	25
VP-a′	CAC ACG GCT TTT GGC TG	4777–4761			
VP-a	**CA**G ATG GGG TTT GCA TCA G	4459–4477	174 (seminested)	95°C, 20 s 57°C, 20 s 72°C, 20 s	35
VP-b′	CAC CGT CCY GTA GCT TTA C	4632–4614			

[a] Boldface indicates mismatched nucleotides which were selected for stability or dimer prevention reasons.
[b] Positions correspond to the GenBank accession M13178.

limit was found to be theoretically ≥5 genome equivalents (geq) per assay, which is equivalent to 250 geq per ml of serum, as calculated on the basis of an external plasmid standard. Optionally, the PCR efficiency can be controlled by an internal amplification control (IC). The benefit of the new method was demonstrated in a child with underlying systemic onset of juvenile idiopathic arthritis (JIA) and relapsing B19 infection, who required an attenuation of immunosuppressive therapy in addition to repeated doses of immunoglobulin to eliminate the virus.

MATERIALS AND METHODS

Patients and serum samples. Immunocompetent patients were grouped on the basis of their B19-specific serostatus irrespective of their disease status: (i) IgM and IgG negative ($n = 30$), (ii) IgG positive and IgM negative ($n = 52$), or (iii) IgM positive ($n = 27$). The sera had been tested for B19-specific IgM and IgG antibodies by an enzyme immunoassay (Medac, Wedel, Germany) which utilized a mixture of baculovirus-expressed recombinant VP-1 and VP-2 B19 proteins. In addition, serum samples ($n = 10$; IgG positive, IgM negative) obtained over a 6-month period from an immunocompromised child with a relapsing B19 infection were examined (see "Case report"). Furthermore, serum samples obtained 15 months before and after the intense 6-month observation period were examined.

Case report. Informed consent was obtained from the parents of the patient prior to publication. An 11-year-old girl had suffered from systemic onset of JIA (also called rheumatoid or chronic arthritis) since the age of 5. Her disease was controlled with a combined immunosuppressive therapy consisting of oral prednisone (0.15 mg/kg daily), subcutaneous methotrexate (20 mg weekly), and oral cyclosporine (5 mg/kg daily). She had a polyarticular bout triggered by an undefined upper respiratory tract infection. To control her symptoms, her dose of prednisone was increased to 1.25 mg/kg daily. One month later, while the prednisone dose was being tapered, the patient contracted another febrile disease. She complained of a dry cough, pain on inspiration, and upper abdominal pain. Her polyarticular symptoms recurred. Later, she developed exertional dyspnea and fatigue. On examination, the patient was afebrile and appeared pale and cushingoid. Her heart rate was 92/min. The edge of the liver was palpable 2 cm below the right costal margin; the spleen was not enlarged. Movement of the cervical spine was limited in all directions, while examination of all other joints revealed no abnormalities.

The differential blood count showed a reticulocytopenic anemia (hemoglobin, 4.4 g/dl; hematocrit, 16%; reticulocyte count, 0.1%). The findings of elevated levels of lactate dehydrogenase (859 U/liter) and total bilirubin (2.0 mg/dl) were consistent with additional hemolysis. The systemic inflammatory parameters, C-reactive protein, haptoglobin, ferritin, fibrinogen, and erythrocyte sedimentation rate were highly elevated, compatible with the exacerbation of her underlying JIA.

The diagnosis was made of a reticulocytopenic anemia with hemolysis, triggering the exacerbation of the underlying rheumatic disease. The serological findings were not useful, since IgG antibodies to parvovirus B19 were present but no specific IgM antibodies were found. However, high titers (3.2×10^9 geq/ml) of parvovirus B19 DNA were detected by PCR in the serum. A serum sample obtained 15 months before onset of the reticulocytopenic anemia tested negative for B19-specific IgM, IgG, and DNA.

DNA extraction. DNA was extracted by a commercial silica-based method (blood kit; Qiagen, Hilden, Germany) from 200 μl of serum samples which had been stored for up to 1 year at −20°C. DNA was eluted with 50 μl of ultrapure water (concentration factor, 4:1). The serum samples had been used before in serological assays; in order to minimize the risk of cross contaminations, care was taken to select sera negative for B19 virus-specific IgM which had not been analyzed in batch with samples that tested IgM positive.

Block cycler-dependent amplification of B19 DNA. Primers for PCR were selected from highly conserved genome regions encoding NS-1 and the structural VP proteins (Table 1). Primers were chosen with the help of Prime software, which is embedded in the GCG package, and the MeltCalc program (41). Amplifications were performed in 50-μl reaction mixtures containing 50 pmol of each primer, 200 μM concentrations of each deoxynucleoside triphosphate, 2 U of HotStar polymerase (Qiagen), and 1.5 mM $MgCl_2$ in the appropriate buffer. The cycling conditions for a T3 block cycler (Biometra, Göttingen, Germany) are shown in Table 1. Amplicons were detected by conventional ethidium bromide-agarose gel electrophoresis.

LC-dependent amplification of B19 DNA. Cycling conditions for primers NS-1a and NS-1a′ were adjusted using SYBR green for detection of amplicons in real time; the specificity of amplicons was evaluated by melting point analysis (FastStart SYBR green kit; Roche Diagnostics). Hybridization probes to be used with the HybProbe LC-FRET technology were selected with the aid of the MeltCalc software (41): probe, 5′-gCA AAA gCC ATT TTA ggC ggg CA-fluorescein; anchor, 5′-LC-Red 640-CAC CAg ggT AgA TCA AAA AAT gCg Tgg A-PO_4 (Fig. 1A). Reaction mixtures of 20 μl were prepared with the FastStart HybProbe kit (Roche Diagnostics) using primers at 20 pmol each and an $MgCl_2$ concentration of 3.0 mM. Probe and anchor were added at 3 pmol each. Sample DNA was added in a volume of 5 μl per reaction. Cycling started with an initial denaturation of 6 min at 96°C followed by 40 cycles of 95°C for 4 s, 56°C for 16 s, and 72°C for 12 s. The temperature for transition from annealing to elongation was lowered from 20 to 2°C per s. Specific hybridization, indicated by the LC-Red 640 signal, was monitored during the annealing phase with the channel setting F2/F1. Fluorimeter gains of the LC were universally set to values of 5 (channel 1), 15 (channel 2), and 30 (channel 3). Melting points for the probe-anchor-target duplexes were checked following completion of the cycling procedure. Hybrids were denatured at 95°C for 10 s, allowed to reanneal at 55°C for 20 s, and then heated at 0.2°C per s to 75°C. Specific products showed a T_m of 64.0°C (±0.5°C) in melting point analysis. The assay was completed within 45 min.

For quantification, each run was performed with five standards calculated to contain theoretically 0.5, 5, 50, 500, and 5,000 copies per assay of a plasmid

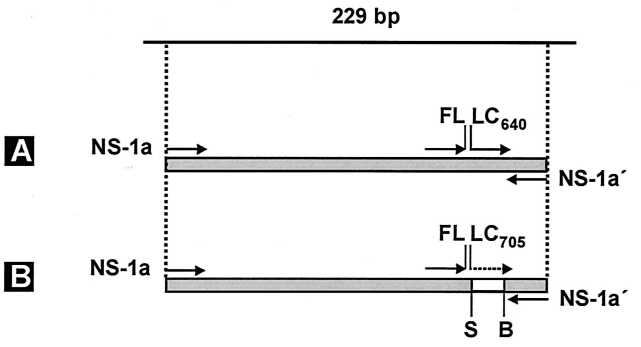

FIG. 1. Amplification and detection of parvovirus B19-specific DNA by using LC-FRET technology. Primers were chosen from the gene encoding NS-1. For primer sequences (NS-1a and NS-1a′) and locations, see Table 1. (A) Detection of the B19-specific amplicon by use of a hybridization probe-and-anchor pair. FL, 3′ fluorescein dye label of the probe; LC_{640}, 5′ LC-Red 640 dye label of the anchor. (B) IC amplicon constructed for coamplification with the specific fragment. S and B, unique *Sph*I and a *Bgl*II sites, respectively, introduced by site-directed mutagenesis. The original anchor sequence between these restriction sites was replaced with a semisynthetic IC sequence (white bar) which can be detected using the IC anchor labeled with LC-Red 705.

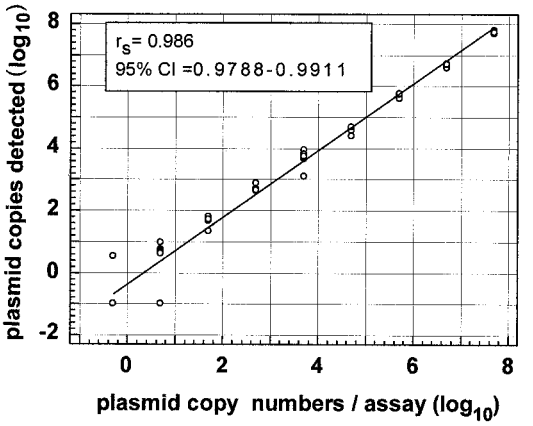

FIG. 2. Performance characteristics of the LC-FRET-dependent amplification of an NS-1-specific fragment of parvovirus B19 DNA. A standard $\log_{10}$ dilution series was prepared from plasmid pPB19N containing the 229-bp NS-1-specific target sequence. Results of up to 14 runs per dilution step are represented. The Spearman rank correlation coefficient (r_s) and the 95% confidence level (CI) are indicated.

harboring the NS-1 gene fragment defined by primers NS-1a and NS-1a′ (pPB19N). Sera which appeared to harbor higher loads of B19 virus DNA were reexamined using an adapted standard dilution series. A negative (water) control was run with all amplifications.

Construction of an IC. An IC was constructed for use in a competitive PCR protocol with the LC-FRET technology. For this purpose, the 229-bp PCR fragment, defined by primers NS-1a and NS-1a′, was cloned into the T/A plasmid vector pCR2.1TOPO (Invitrogen, Groningen, The Netherlands) to give the plasmid pPB19N. The fragment was mutated using the QuickChange kit (Stratagene, La Jolla, Calif.) to accept unique *Sph*I and *Bgl*II sites flanking the sequence of the anchor probe (Fig. 1B). The mutated fragment was transferred into the *Eco*RI site of the vector pGEM 9Zf(+) (Promega, Madison, Wis.), which does not contain *Sph*I or *Bgl*II sites. The original HybProbe anchor sequence was replaced, after *Sph*I/*Bgl*II double digestion, with a synthetic sequence (plasmid pPBIC). Detection of IC amplicons generated with primers NS-1a and NS-1a′ was then carried out by means of the B19-specific fluorescein-labeled probe described above and the unique IC anchor 5′-LC-Red 705-CAC gCT CAC AgC gCA gTA gAT CT-PO_4 measured at channel 3 of the LC (band-pass, 710 nm).

DNA quantification. Quantities and copy numbers of plasmid pPB19N and pPBIC were calculated following UV spectrophotometry (260 nm) and by gel electrophoresis against a standardized size ladder (SmartLadder; Eurogentech, Seraing, Belgium).

Parvovirus B19 isolate V9. Plasmid DNA which harbored a large part of the entire genomic DNA of the B19 isolate V9 (38), including the NS-1 and VP gene sequences targeted by our PCRs, was kindly supplied by Q. T. Nguyen, Institut Pasteur, Paris, France.

Statistical analysis. The strength of agreement between the results of different assays was measured by robust kappa (κ) statistics (18), implemented, e.g., in the EpiInfo 6.0 software distributed by the World Health Organization and Centers for Disease Control and Prevention. According to convention, a κ coefficient of >0.6 indicated good agreement, whereas a κ of >0.8 signaled very good agreement.

RESULTS

Performance characteristics of the B19 LC PCR. A standard dilution of B19-specific sequence copies was prepared using plasmid pPB19N, which contains a 229-bp fragment of the NS-1 gene generated by PCR using the primer pair NS-1a–NS-1a′ (Table 1). Serial 10-fold dilutions were made in diethyl pyrocarbonate-treated water containing 2 mg of denatured herring sperm DNA $liter^{-1}$ as a stabilizer. Aliquots of 5 μl were analyzed for B19 DNA.

Quantification using the LC-FRET PCR was feasible with acceptable reproducibility over a wide dynamic range of 7 $\log_{10}$ steps to as little as theoretically ≥5 geq per assay (Fig. 2). Up to 14 measurements per log step were run separately from the same master dilution series over a period of 8 weeks in order to assess reproducibility. The relative standard deviation (%SD) within and between the different runs was generally below 30%, except for dilutions containing theoretically 5 (%SD = 62) and 0.5 (%SD = 265) geq per assay. In 4 of 13 runs with samples containing theoretically 0.5 geq per assay, amplicons were not detected in real time, but a weak though specific T_m signal at 64.0°C was obtained during melting point analysis. These samples were regarded as qualitatively positive but not quantifiable. Therefore, both detection and quantification of theoretically 0.5 geq per assay were regarded as unreliable.

With the availability of two different anchor labels, i.e., LC-Red 640 and 705, simultaneous monitoring for a specific product and an IC is possible. We constructed an IC plasmid (pPBIC) with a unique semisynthetic control sequence which is coamplified with the specific product and detected by an LC-Red 705-labeled IC anchor (Fig. 1B). On the basis of this competitive PCR protocol, the IC can be used to monitor inhibitory substances which might have been copurified with the sample DNA. Although care was taken to select anchors specific for the IC or the NS-1 fragment with comparable hybridization properties, the IC was detected with lower sensitivity (data not shown). Therefore, 200 copies of the IC plasmid had to be spiked per assay for its reliable detection, and this resulted in a decrease of the sensitivity of the B19 virus-specific LC-FRET PCR by 1 log step to theoretically 50 B19 virus geq per assay.

Detection of the genetically diverse human erythrovirus isolate V9. Recently, a genetically markedly distinct erythrovirus isolate (termed V9) was detected in a child with transient aplastic anemia (38). The authors reported an estimated se-

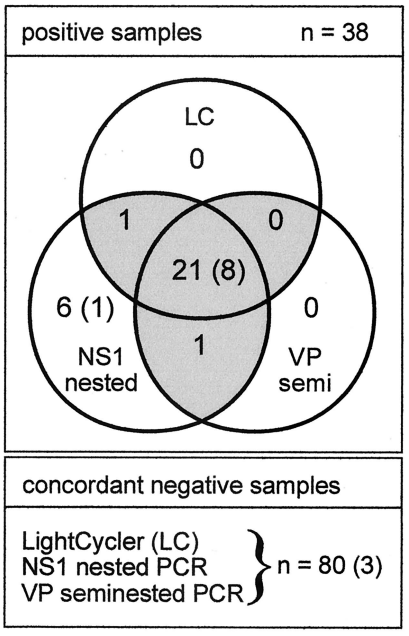

FIG. 3. Detection of parvovirus B19 DNA in patient serum samples by three different DNA amplification methods. LC, LC-FRET assay specific for a 229-bp fragment of the NS-1 locus; VP, seminested PCR specific for a 174-bp fragment of the VP-1 locus; NS1, nested PCR specific for a 99-bp fragment of the NS-1 locus. Shaded areas of the Venn diagram indicate samples which were concordantly positive by at least two PCR formats. Numbers in parentheses indicate serum samples from an immunocompromised child; other samples originated from immunocompetent individuals.

quence divergence from standard B19 strains of at least 15% in some regions. A plasmid containing large parts of the genomic DNA of the V9 isolate was tested in our various PCR formats. Specific amplicons were obtained with the NS-1-specific block cycler PCR and with the LC-FRET assays but not with the seminested VP-1 PCR (data not shown).

Comparative analysis of patient sera for B19 DNA. A total of 109 sera from 102 immunocompetent patients and 12 sera from the immunocompromised child with JIA were examined in three different PCRs. The results are summarized in Fig. 3 (Venn diagram). All samples from immunocompetent patients which yielded a positive PCR result that was concordantly positive between at least two formats (grey portions of the Venn diagram) also proved to be positive for B19 IgM. These patients presented with typical symptoms of acute B19 infection. By nested NS-1 PCR, six additional sera from immunocompetent patients tested positive. Three of these also tested IgM positive, while the remaining three came from the IgG^+ IgM^- cohort. None of the seronegative patients tested positive in either PCR format. An additional eight sera from the immunocompromised child (IgG^+ IgM^-) with relapsing B19 infection tested concordantly positive in all three PCR formats, while one sample from this child was positive by nested NS-1 PCR only, and three sera were concordantly negative. Interrater analysis (kappa statistics [18]) indicated a very good agreement (conventional definition, $\kappa > 0.8$) between the LC-FRET PCR and the nested NS-1 as well as the seminested VP PCR ($\kappa = 0.85$ and 0.98, respectively). Therefore, the LC-FRET PCR can be used as a substitute for both the nested NS-1 and the seminested VP-1 PCRs.

The kappa statistics also indicated a very good agreement between the qualitative LC-FRET PCR results and the IgM serostatus ($\kappa = 0.92$) when sera of immunocompetent patients were considered. The quantifiable virus loads detected by the LC-FRET PCR in patient samples ranged between theoretically 50 and 3.2×10^9 geq per ml of serum.

B19 DNA loads and clinical course of a relapsing infection in an immunocompromised child. Based on the detection of B19 DNA in serum, the diagnosis of an acute parvovirus B19 infection (Fig. 4) with aplastic crisis was made in a child who required immunosuppressive therapy for underlying systemic onset of JIA. Initially, the B19 DNA load peaked at 3.2×10^9 geq per ml serum (Fig. 4, day 0). Circulatory compromise occurred and the patient received two packs of red blood cells. The ongoing severe systemic inflammatory activity did not allow discontinuation of the immunosuppressive therapy at that point. To specifically treat the B19 infection, the patient received a 5-day-course of polyvalent intravenous (i.v.) IgG (400 mg/kg daily). The reticulocytopenic anemia resolved within a week. The polyarticular symptoms subsided shortly after the diagnosis of acute parvovirus infection was made and the prednisone dose was tapered (day 10). B19 DNA loads decreased below the detection level (by LC-FRET PCR) in the serum within 2 months (day 60), suggesting a gradual clearance of the virus from these compartments (Fig. 4). The serum obtained at day 60 tested positive for B19 DNA only by the nested NS-1 PCR.

Two months after initial diagnosis of an acute parvovirus B19 infection (day 60), the patient had another polyarticular relapse. The first features of the relapse, raised systemic inflammatory markers, were obvious on day 30, and the patient required an increase of the prednisone dose to 1.25 mg/kg daily. In addition, high-dose methotrexate was given intravenously (1 mg/kg weekly). Six weeks after the immunosuppressive therapy was intensified (day 88), the reticulocytopenic anemia relapsed (hemoglobin, 9.0 g/dl; hematocrit, 31%; reticulocyte count, 0.1%) and B19 DNA recurred in the serum, this time peaking at 6×10^6 geq per ml of serum (Fig. 4). The clinical diagnosis of a recurrent parvovirus B19 infection associated with pure red cell anemia was made. To accelerate viral elimination, monthly high-dose immunoglobulin therapy (1.5 mg/kg) was started. In spite of the immunoglobulin therapy, B19 DNA was continuously detected. Ultimately, the polyarticular symptoms came into clinical remission, allowing tapering of the immunosuppressive therapy. Cyclosporine was discontinued, and prednisone was further tapered. No clinically overt relapse of the B19 infection occurred for a follow-up period of 12 months, coincident with serum viral loads declining below the detection level when tested with both the LC-FRET and the nested NS-1 PCR assays. A sustained negative B19 DNA status was confirmed when a serum sample obtained 15 months later also tested negative. The underlying rheumatic disease is in clinical remission.

DISCUSSION

We have developed a rapid quantitative PCR assay, based on LC-FRET technology, for the detection of B19 DNA.

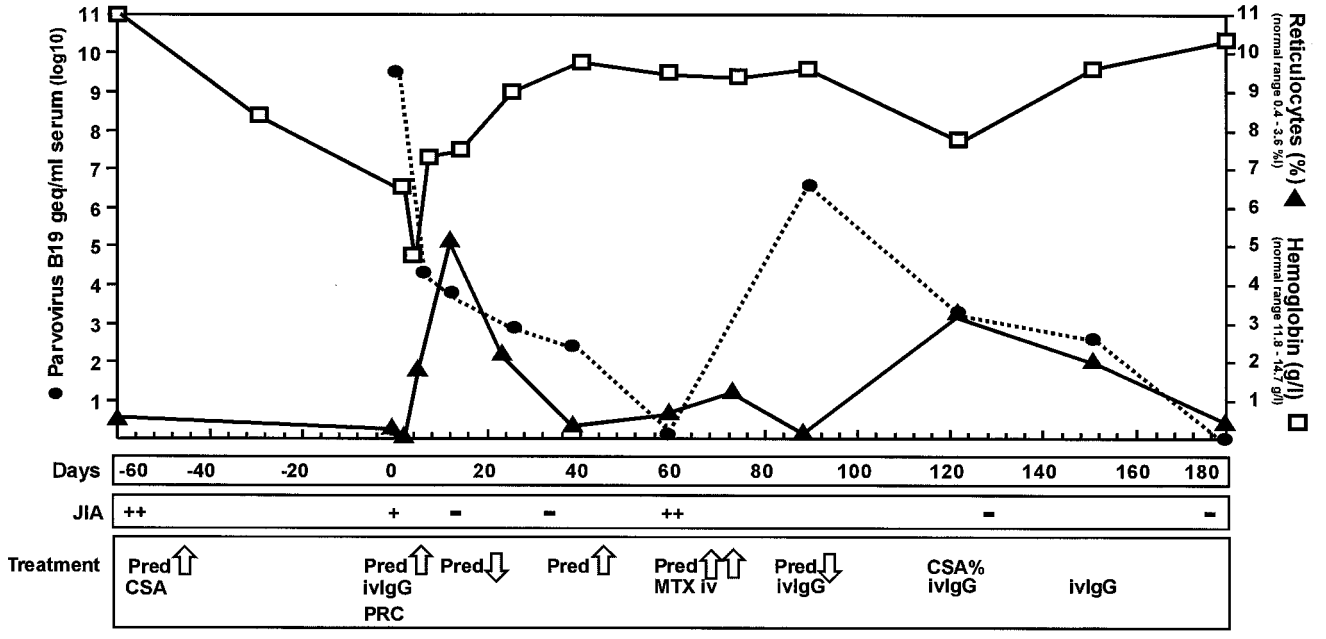

FIG. 4. Kinetics of the parvovirus B19 DNA load in serum, hemoglobin values, and reticulocyte counts in an immunosuppressed child with underlying systemic onset of JIA (++, severe symptoms; +, moderate symptoms; −, no symptoms) and relapsing B19 infection. Day 0 indicates the first PCR-based diagnosis of an active B19 infection. B19 genome equivalents were calculated on the basis of an external plasmid standard. Treatments include packed red cells (PRC), prednisone (Pred; arrows indicate an increasing or decreasing dose), i.v. IgG containing antibodies specific for B19 VP-1, i.v. methotrexate (MTX), and discontinuation of cyclosporine (CSA%), as part of the immunosuppressive regimen.

Quantification of viral DNA loads in serum was possible over a dynamic range of 7 log steps down to the limit of theoretically 250 geq per ml of serum. Lower virus loads were detected unreliably and by melting point analysis only. False-negative results can be controlled by coamplification of an internal standard, albeit at the expense of a loss of sensitivity of 1 log step (Fig. 2).

LC-FRET was used to detect B19 DNA in serum samples from immunocompetent patients selected on the basis of their B19-specific serostatus, and the results were compared to those of two conventional block cycler PCR formats (nested NS-1-specific and seminested VP-specific PCR). The nested NS-1 PCR proved to be more sensitive, since an additional six sera tested positive by this assay only (Fig. 3). This reflects the performance characteristics of the nested NS-1 PCR when tested with the positive control plasmid pPBN19 (data not shown). Samples which tested concordantly positive by at least two different PCR formats were also positive for B19 IgM (Fig. 3). Both LC-FRET and the VP PCR failed to identify six sera of which three also tested positive for B19 IgM. An additional three sera which tested DNA positive by the nested NS-1 PCR exclusively, however, came from immunocompetent IgM-negative IgG-positive patients with no clinical signs of B19 infection. It remains to be clarified whether these results are due to a prolonged viremic but asymptomatic infection or represent false-positive results. Despite these discrepancies, the kappa coefficient revealed a very good correlation between the LC-FRET PCR and the block cycler PCR formats. The sensitivity of the LC-FRET PCR is in the range of other published B19 DNA quantification methods, i.e., approximately 5 geq per assay (1, 4, 10, 17, 22, 25, 40). For immunocompetent patients, LC-FRET PCR also correlated favorably with IgM serostatus ($\kappa = 0.92$).

Genetic variation between B19 wild-type isolates has been reported to be less than 5%, and few genetic changes accumulate longitudinally during prolonged chronic infection in individual patients (27). Our primers and probes were positioned in regions which were completely conserved between at least five different isolates for which sequence data were available from the databases. DNA derived from the human erythrovirus isolate V9, which was reported to be genetically divergent from standard B19 wild-type strains (38), was readily detected by our NS-1-specific PCRs (LC and nested NS-1) but not by the VP-specific seminested PCR.

The reported case of the immunosuppressed child with underlying systemic onset of JIA and relapsing parvovirus B19 infection is an example of the new method's value in therapeutic decision-making. The child experienced two separate episodes of active B19 replication, which could be quantitatively monitored and clearly discerned only by the LC-FRET PCR (Fig. 4) but not by the nested NS-1 PCR, which also yielded a positive signal for the serum obtained at day 60. Therapeutic interventions were guided by the quantification of viral loads in the serum in association with the hematological values. Treatment with i.v. IgG, combined with an attenuated T-cell-suppressive regimen, finally led to a stable hematologic state with viral loads below the detection level of the LC-FRET PCR.

Immunosuppressive therapy, e.g., in autoimmune diseases, is considered a risk factor for persistence of the parvovirus B19 (7). Immunocompromised patients have difficulties eliminating the virus from their bone marrow, and bone marrow insuffi-

ciency may persist for up to 10 years (31). Chronic infections without underlying immunodeficiencies are rarely described (16, 35, 37). Protection from parvovirus B19 is thought to be mediated by neutralizing antibodies (32, 49). Specific IgM antibodies are detectable as early as day 5 after infection and persist for months, while IgG antibodies are detectable from the second week postinfection and have lifelong persistence (49). Neutralizing antibodies are mounted against both capsid proteins VP-1 and VP-2 (3, 21, 39, 48). Antibodies against VP-1, the minor capsid protein, are found predominantly in convalescent-phase sera (32, 49). Antibodies against VP-2, the major capsid protein, are found predominantly during the acute disease and early convalescence (26, 32, 42), especially when denatured (linear) antigen is used in the test system. However when native (conformational) VP2 antigen is used, the antibodies can also be detected in convalescent-phase sera (28, 42). A deficiency in generating specific antibodies either qualitatively (e.g., patients with congenital or acquired immunodeficiencies) or quantitatively (e.g., patients with leukemia) is considered responsible for persistent B19 infections (32, 49). Consequently, supplementation of specific immunoglobulins is the accepted therapy of choice (29, 30, 32, 33, 49). Commercial preparations of immunoglobulins contain specific parvovirus B19 antibodies, which are deemed responsible for clinical effectiveness. We tested one lot of the immunoglobulins given to our patient (Sandoglobin; Novartis, Nürnberg, Germany) and detected B19 VP-specific antibodies by enzyme-linked immunosorbent assay (Medac). The standard dose of i.v. IgG is 400 mg/kg daily for 5 to 10 days (29, 49). In our patient, i.v. IgG treatment coincided with declining viral loads in the serum (Fig. 4) but obviously failed to eliminate the virus from the bone marrow, as was evident from the rebound of viral DNA loads associated with reticulocytopenia while the patient was under intensified immunosuppressive treatment. In AIDS patients with relapses of B19 infection, i.v. IgG is given at monthly intervals at a dosage of 1 g/kg daily for 1 to 2 days (30). We adapted the protocol accordingly. Again, i.v. IgG treatment led to gradually declining viral loads in serum, but only when the T-cell-suppressive regimen was attenuated by tapering the prednisone and discontinuing cyclosporine, in addition to repeated doses of immunoglobulins, did we observe a sustained hematological normalization and undetectable viral loads in serum.

The patient's course allows speculations about the relative importance of the humoral and cellular immune responses in persistent parvovirus infection. In general, neutralizing antibodies are thought to be the mainstay of acquired immunity (32, 49). Only recently has it become evident that cellular immunity plays a significant role in overcoming acute infection and providing long-term memory (20, 46, 45). When our patient had her first episode of parvovirus infection, a standard dose of immunoglobulins suppressed the DNA levels below the detection limit but did not eliminate the virus. The infection relapsed after the prednisone dose, a potent inhibitor of T-cell function, was increased. Immunoglobulin therapy was reinstituted. Four weeks after reinstitution of i.v. IgG therapy, the viral load declined by a factor of 4×10^3. Immunoglobulin therapy after the first episode had led to a decline of viral DNA load by a factor of 5×10^6. We therefore reasoned that immunoglobulin therapy might not be sufficient to clear the virus, and we attenuated the immunosuppressive regimen. In parallel, i.v. IgG therapy was continued. This two-pronged therapeutic approach allowed the patient to finally clear the virus from circulation. After more than 15 months, B19 DNA remained undetectable in serum. In retrospect, it is not possible to ascribe the effect of viral elimination to either attenuation of T-cell suppressive therapy or to repeated doses of immunoglobulins.

In conclusion, the LC-FRET PCR specific for B19 DNA can substitute for conventional nested PCR formats for the diagnosis of an active B19 infection. The advantages of the LC-FRET PCR are its rapidity (45 min versus 5 h), ease of preparation (one tube, including, if desired, an IC), diminished risk of cross contamination, high specificity, and the option of quantification. Given the reduced hands-on time, implementation of this format would appealingly allow cost reduction in the clinical diagnostic laboratory. The LC-FRET PCR can guide the therapeutic options of repeated immunoglobulin therapy versus a reduction of immunosuppressive regimens in patients with persistent parvovirus infections.

ACKNOWLEDGMENTS

We thank Bianca Grafelmann-Hilali and Helga Janeçek for technical assistance and Carolyn Cannon for reviewing the manuscript, and we gratefully acknowledge the help of Q. T. Nguyen in supplying erythrovirus V9-specific sequences.

T.C.H. and M.H. contributed equally to this work.

REFERENCES

1. **Aberham, C., C. Pendl, P. Gross, G. Zerlauth, and M. Gessner.** 2001. A quantitative, internally controlled real-time PCR assay for the detection of parvovirus B19 DNA. J. Virol. Methods **92:**183–191.
2. **Abkowitz, J. L., K. E. Brown, R. W. Wood, N. L. Kovach, S. W. Green, and N. S. Young.** 1998. Clinical relevance of parvovirus B19 as a cause of anemia in patients with human immunodeficiency virus infection. J. Infect. Dis. **176:**269–273.
3. **Arakelov, S., M. K. Gorny, C. Williams, C. H. Riggin, F. Brady, M. C. Collet, and S. Zolla-Pazner.** 1993. Generation of neutralizing anti-B19 parvovirus human monoclonal antibodies from patients with human immunodeficiency virus. J. Infect. Dis. **168:**580–585.
4. **Aubin, J. T., C. Defer, M. Vidaud, M. Maniez Montreuil, and B. Flan.** 2000. Large-scale screening for human parvovirus B19 DNA by PCR: application to the quality control of plasma for fractionation. Vox Sang. **78:**7–12.
5. **Broliden, K., T. Tolfvenstam, S. Ohlsson, and J. I. Henter.** 1998. Persistent B19 parvovirus infection in pediatric malignancies. Med. Pediatr. Oncol. **31:**66–72.
6. **Brown, K. E., S. M. Anderson, and N. S. Young.** 1993. Erythrocyte P antigen: cellular receptor for B19 parvovirus. Science **262:**115–117.
7. **Brown, K. E., and N. S. Young.** 1997. Parvovirus B19 in human disease. Annu. Rev. Med. **48:**59–64.
8. **Brown, K. E.** 2000. Haematological consequences of parvovirus B 19 infection. Bailliere's Best Pract. Res. Clin. Haematol. **13:**245–259.
9. **Carriere, C., P. Boulanger, and C. Delsert.** 1993. Rapid and sensitive method for the detection of B19 virus DNA using the polymerase chain reaction with nested primers. J. Virol. Methods **44:**221–234.
10. **Cassinotti, P., and G. Siegl.** 2000. Quantitative evidence for persistence of human parvovirus B19 DNA in an immunocompetent individual. Eur. J. Clin. Microbiol. Infect. Dis. **19:**886–887.
11. **Dieck, D., R. L. Schild, M. Hansmann, and A. M. Eis-Hübinger.** 1999. Prenatal diagnosis of congenital parvovirus B19 infection: value of serological and PCR techniques in maternal and fetal serum. Prenatal Diagn. **19:**1119–1123.
12. **Druschky, K., J. Walloch, J. Heckmann, B. Schmidt, H. Stefan, and B. Neundorfer.** 2000. Chronic parvovirus B-19 meningoencephalitis with additional detection of Epstein-Barr virus DNA in the cerebrospinal fluid of an immunocompetent patient. J. Neurovirol. **6:**418–422.
13. **Durigon, E. L., D. D. Erdman, G. W. Gary, M. A. Pallansch, T. J. Török, and L. J. Anderson.** 1993. Multiple primer pairs for polymerase chain reaction (PCR) amplification of human parvovirus B19 DNA. J. Virol. Methods **44:**155–165.
14. **Eis-Hübinger, A. M., D. Dieck, R. Schild, M. Hansmann, and K. E. Schneweis.** 1998. Parvovirus B19 infection in pregnancy. Intervirology **41:**178–184.
15. **Erdman, D. D., E. L. Durigon, and B. P. Holloway.** 1994. Detection of human

parvovirus B19 DNA PCR products by RNA probe hybridization enzyme immunoassay. J. Clin. Microbiol. **32:**2295–2298.
16. **Faden, H., G. W. Gary, and L. J. Anderson.** 1992. Chronic parvovirus infection in a presumably immunologically healthy woman. Clin. Infect. Dis. **15:**595–597.
17. **Fini, F., G. Gallinella, S. Girotti, M. Zerbini, and M. Musiani.** 1999. Development of a chemiluminescence competitive PCR for the detection and quantification of parvovirus B19 DNA using a microplate luminometer. Clin. Chem. **45:**1391–1396.
18. **Fleiss, J. L.** 1981. The measurement of interrater agreement, p. 212–236. *In* J. L. Fleiss (ed.), Statistical methods for rates and proportions. Wiley, New York, N.Y.
19. **Flunker, G., A. Peters, S. Wiersbitzky, S. Modrow, and W. Seidel.** 1998. Persistent parvovirus B19 infections in immunocompromised children. Med. Microbiol. Immunol. (Berlin) **186:**189–194.
20. **Franssila, R., K. Hokynar, and K. Hedman.** 2001. T helper cell-mediated in vitro responses of recently and remotely infected subjects to a candidate recombinant vaccine for human parvovirus B19. J. Infect. Dis. **183:**805–809.
21. **Gigler, A., S. Dorsch, A. Hemauer, C. Williams, S. Kim, N. S. Young, S. Zolla-Panzer, H. Wolf, M. K. Gorny, and S. Modrow.** 1999. Generation of neutralizing human monoclonal antibodies against parvovirus B19 proteins. J. Virol. **73:**1974–1979.
22. **Gruber, F., F. G. Falkner, F. Dorner, and T. Hämmerle.** 2001. Quantitation of viral DNA by real-time PCR applying duplex amplification, internal standardization, and two-color fluorescence detection. Appl. Environ. Microbiol. **67:**2837–2839.
23. **Heegaard, E. D., and A. Hornsleth.** 1995. Parvovirus: the expanding spectrum of disease. Acta Paediatr. **84:**109–117.
24. **Hemauer, A., A. Gigler, K. Searle, K. Beckenlehner, U. Raab, K. Broliden, H. Wolf, G. Enders, and S. Modrow.** 2000. Seroprevalence of parvovirus B19 NS1-specific IgG in B19-infected and uninfected individuals and in infected pregnant women. J. Med. Virol. **60:**48–55.
25. **Hornsleth, A., K. M. Carlsen, L. S. Christensen, M. Gundestrup, E. D. Heegaard, and J. Myhre.** 1994. Estimation of serum concentration of parvovirus B19 DNA by PCR in patients with chronic anaemia. Res. Virol. **145:**379–386.
26. **Kaikkonen, L., H. Lankinen, I. Harjunpää, K. Hokynar, M. Söderlund-Venermo, C. Oker-Blom, L. Hedman, and K. Hedman.** 1999. Acute-phase-specific heptapeptide epitope for diagnosis of parvovirus B19 infection. J. Clin. Microbiol. **37:**3952–3956.
27. **Kerr, J. R., M. D. Curran, J. E. Moore, and P. G. Murphy.** 1995. Parvovirus B19 infection—persistence and genetic variation. Scand. J. Infect. Dis. **27:** 551–557.
28. **Kerr, S., G. O'Keeffe, C. Kilty, and S. Doyle.** 1999. Undenatured parvovirus B19 antigens are essential for the accurate detection of parvovirus B19 IgG. J. Med. Virol. **57:**179–185.
29. **Koch, W. C., G. Massey, C. E. Russell, and S. P. Adler.** 1990. Manifestations and treatment of human parvovirus B19 infection in immunocompromised patients. J. Pediatr. **116:**355–359.
30. **Koduri, P. R., R. Kumapley, J. Valladares, and C. Teter.** 1999. Chronic pure red cell aplasia caused by parvovirus B19 in AIDS: use of intravenous immunoglobulin—a report of eight patients. Am. J. Hematol. **61:**16–20.
31. **Kurtzman, G. J., K. Ozawa, B. Cohen, G. Hanson, R. Oseas, and N. S. Young.** 1987. Chronic bone marrow failure due to persistent B19 parvovirus infection. N. Engl. J. Med. **317:**287–294.
32. **Kurtzman, G. J., B. J. Cohen, A. M. Field, R. Oseas, R. M. Blaere, and N. S. Young.** 1989. Immune response to B19 parvovirus and an antibody defect in persistent viral infection. J. Clin. Investig. **84:**1114–1123.
33. **Kurtzman, G. K., N. Frickhofen, J. Kimball, D. W. Jenkins, A. W. Nienhuis, and N. S. Young.** 1989. Pure red cell aplasia of 10 years' duration due to persistent parvovirus B19 infection and its cure with immunoglobulin therapy. N. Engl. J. Med. **321:**519–525.
34. **Lundqvist, A., T. Tolfvenstam, M. Brytting, C. M. Stolt, K. Hedman, and K. Broliden.** 1999. Prevalence of parvovirus B19 DNA in bone marrow of patients with haematological disorders. Scand. J. Infect. Dis. **31:**119–122.
35. **Lundqvist, A., T. Tolfvenstam, J. Bostic, M. Soderlund, and K. Broliden.** 1999. Clinical and laboratory findings in immunocompetent patients with persistent parvovirus B19 DNA in bone marrow. Scand. J. Infect. Dis. **31:** 11–16.
36. **Moore, T. L.** 2000. Parvovirus-associated arthritis. Curr. Opin. Rheumatol. **12:**289–294.
37. **Murray, J. C., M. V. Greisik, F. Leger, and K. L. McClain.** 1993. B19 Parvovirus induced anemia in a normal child. Am. J. Pediatr. Hematol. Oncol. **15:**420–423.
38. **Nguyen, Q. T., C. Sifer, V. Schneider, X. Allaume, A. Servant, F. Bernaudin, V. Auguste, and A. Garbarg-Chenon.** 1999. Novel human erythrovirus associated with transient aplastic anemia. J. Clin. Microbiol. **37:**2483–2487.
39. **Sato, H., J. Hirata, N. Kuroda, H. Shiraki, Y. Maeda, and K. Okochi.** 1991. Identification and mapping of neutralizing epitopes of human parvovirus B19 by using human antibodies. J. Virol. **65:**5485–5490.
40. **Sato, K., E. Matsuda, K. Kamisango, H. Iwasaki, S. Matsubara, and Y. Matsunaga.** 2000. Development of a hypersensitive detection method for human parvovirus B19 DNA. J. Clin. Microbiol. **38:**1241–1243.
41. **Schütz, E., and N. von Ahsen.** 1999. Spreadsheet software for thermodynamic melting point prediction of oligonucleotide hybridization with and without mismatches. BioTechniques **27:**1218–1228.
42. **Söderlund, M., C. S. Brown, W. J. M. Spaan, L. Hedman, and K. Hedman.** 1995. Epitope type-specific IgG responses to capsid proteins VP1 and VP2 of human parvovirus B19. J. Infect. Dis. **172:**1431–1436.
43. **Stiefel, L.** 1995. Erythema infectiosum (fifth disease). Pediatr. Rev. **16:**474–475.
44. **Takahashi, Y., C. Murai, S. Shibata, Y. Munakata, T. Ishii, K. Ishii, T. Saitoh, T. Sawai, K. Sugamura, and T. Sasaki.** 1998. Human parvovirus B19 as a causative agent for rheumatoid arthritis. Proc. Natl. Acad. Sci. USA **95:**8227–8232.
45. **Tolfvenstam, T., A. Oxenius, D. A. Price, B. L. Shacklett, H. M. L. Spiegel, K. Hedman, O. Norbeck, M. Levi, K. Olsen, M. Kantzanou, D. F. Nixon, K. Broliden, and P. Klenerman.** 2001. Direct ex vivo measurement of CD8+ T-lymphocyte responses to human parvovirus B19. J. Virol. **75:**540–543.
46. **von Poblotzki, A., C. Gerdes, U. Reischl, H. Wolf, and S. Modrow.** 1996. Lymphoproliferative responses after infection with human parvovirus B19. J. Virol. **70:**7327–7330.
47. **Wittwer, C. T., K. M. Ririe, R. V. Andrew, D. A. David, R. A. Gundry, and C. J. Balis.** 1997. The LightCycler: a microvolume multisample fluorimeter with rapid temperature control. BioTechniques **22:**176–181.
48. **Yoshimoto, K., S. Rosenfeld, N. Frickhofen, D. Kennedy, R. Hills, S. Kajigaya, and N. S. Young.** 1991. A second neutralizing epitope of B19 parvovirus implicates the spike region in the immune response. J. Virol. **65:**7056–7060.
49. **Young, N. S.** 1996. Parvovirus infection and its treatment. Clin. Exp. Immunol. **104**(Suppl. 1)**:**26–30.